



Broadband plus-shaped metasurface absorber based on graphene for visible and ultraviolet regions

K. E. Lakshmiprabha¹ · C. Govindaraju² · G. Mahendran³

Received: 18 April 2022 / Accepted: 1 September 2022 / Published online: 29 September 2022
© The Author(s), under exclusive licence to Springer Science+Business Media, LLC, part of Springer Nature 2022

Abstract

Solar energy absorption for the whole spectral irradiance is important which includes UV, visible and infrared regions. We have proposed a new metasurface solar absorber design by optimizing the different metasurface designs to absorb most of the solar radiation. The design results are obtained for two metasurface designs namely plus-shape metamaterial design and I-shape metamaterial design. The absorption result comparison of these two designs clearly shows that the plus-shape metamaterial design is having more absorption for all three regions. The highest average absorption of 95% is observed for the visible region for plus-shape metamaterial design. The design results for different parameter variations such as thickness, width, length, etc. are observed and an optimized design is obtained. The design results for the angle of incidence are also observed which clearly shows that the design is having a wide angle of incidence. The graphene potential variation is not affecting the overall absorption of the design. The proposed solar absorber with its wide angle of incidence and high absorption in the solar spectrum can be used for solar thermal energy conversion applications.

Keywords Absorber · Renewable energy · Metasurface · Graphene

1 Introduction

The demand for energy is rising, and clean and renewable energy sources are needed because fossil fuels are limited and polluting our environment. Renewable energy is gaining interest among researchers because they are non-polluting and available in abundance. Renewable energy uses natural resources like wind, solar, water, etc. (Elavarasan et al. 2020; Bait-Suwallam et al. 2019). One of the most effective renewable energy sources is solar energy because solar energy is available easily and if the efficiency of the solar cells/absorbers can be improved then the need for energy in the world can be resolved. The solar

✉ K. E. Lakshmiprabha
lakshmiprabha.ethirajan@gmail.com

¹ Karpaga Vinayaga College of Engineering and Technology, Chengalpattu (D.T) 603308, India

² Government College of Engineering, Salem 636011, India

³ Kathir College of Engineering, Coimbatore 641062, India

absorber captures solar radiation energy and transforms it into heat or electricity (Wang et al. 2015; Rufangura and Sabah Oct. 2015). The solar absorber is an efficient way for solar thermal energy conversion which can be applied to many solar applications (Li et al. 2020). The solar absorber radiation is absorbed in three solar spectral regions namely infrared, visible and ultraviolet regions. The broadband absorption can be achieved with the use of metamaterial, graphene, etc. (Patel et al. 2019a). Metamaterials can be used to improve absorption by reducing tungsten nanowires (Bilal et al. 2020).

Metamaterials are artificial materials having a negative refractive index which improves different performance parameters of the solar absorbers (Patel et al. 2020). Broadband absorption is one of the important parameters which can be improved by incorporating metamaterials in the solar absorber designs (Xu et al. 2019; Mehrabi et al. 2020; Jadeja et al. 2020; Patel et al. 2021a, 2022). The broadband absorption can be achieved with a reduction in the unit cell area. Solar absorber design is optimized for better performance in Heidari and Sedighy (2018). Metamaterials are effective in increasing the absorption as well as increasing the sensitivity of the sensors. The sensitivity of the sensors which is observed through its high absorption peaks for different concentrations can also be enhanced using metamaterials (Parmar and Patel 2021). Terahertz metasurface absorbers are also applicable in thermal applications (Chen et al. 2020; Cheng et al. 2020, 2021a). Broadband metasurface absorbers can be designed with square ring-shaped resonators (Cheng et al. 2021b). Perfect absorbers can also be used for sensing applications (Zhang et al. 2021; Cheng et al. 2021c).

Graphene is a single atom thick graphite material having outstanding electrical and optical qualities. The characteristics of graphene can be employed to enhance absorbers' absorption (Patel et al. 2019b). The optical properties of the graphene material help in achieving these applications. Graphene materials also help in absorbing radiation in the THz regime (Feng et al. 2021). Graphene-based absorbers are gaining interest amongst researchers because of their wide applicability which includes THz applications and solar absorbers (Patel et al. 2020; Parmar and Patel 2021). To increase the solar absorber's absorption, two distinct metasurface forms are used in the design of absorber. Machine learning methods are used to improve the absorber results (Parmar et al. 2022). Graphene material is used with its patterned design with metamaterials to get the electrical tuning and easier fabrication in broadband absorber (Han and Chen 2020). The three-dimensional structured graphene metamaterial (SGM) can be a good pick because of its metallic trench-like structure's wavelength selectivity. The ultrathin graphene metamaterial layer has high heat conductivity and a broadband dispersion-less nature as a result (Lin et al. 2020). A Broadband solar absorber using graphene metasurface is designed to absorb the visible region. The absorber is enhancing the absorption using graphene metasurface (Charola et al. 2020). The graphene-based absorber is giving a wide angle of incidence with polarization insensitiveness (Rahmanzadeh et al. 2018). Graphene metal absorbers can be used to tune the spectrum of the terahertz absorbers. Various design characteristics can be changed to achieve this adjustment with graphene chemical potential (Torabi et al. Mar. 2017; Patel et al. 2021b). The solar absorbers are applicable for heating residential/commercial buildings. One of the most important applications is industrial heating. Solar thermal energy is also applicable in photovoltaics. Solar absorbers are also applicable in power generation (Han et al. 2016; Zhang et al. 2022; AL-Rjoub et al. 2018).

The need for accommodating the visible regions with the ultraviolet region and infrared region is increasing day by day so We have proposed a solar absorber that is absorbing most of the solar energy with high efficiency. The design is further improved by tracking the effects of various adjustments in physical factors such as substrate length, width, and

height. The electric field of the design is also observed to verify the absorption behavior for different wavelengths. The design and modeling, results and analysis, and conclusion are presented in Section-II, Section-III, and Section-IV respectively.

2 Solar absorber design

The absorber is designed by placing a plus shape metamaterial shape above the silicon dioxide substrate with a graphene spacer layer is displayed in Fig. 1. The structure is having Titanium material as a metasurface resonator. The design of the plus-shape metamaterial is shown in the figure. The design is verified for two different variants of the design namely the I-shape design and the Plus-shape design. Two designs are verified to check the best performance of the plus shape design over the other design. The design parameters like length, width and thickness are varied to optimize the design. The optimum design is designed based on this variation and the optimum design is having substrate thickness = $2.5 \mu\text{m}$, substrate length and width = $2 \mu\text{m}$. Graphene layer thickness is 0.34 nm , resonator thickness is $0.2 \mu\text{m}$, and resonator breadth is 120 nm . To enhance the absorption capabilities of the suggested solar absorber, graphene materials is used. The metasurface design show plus-shape sign from the top as shown in Fig. 1a where the graphene layer is visible below the plus-shape metamaterial. The front view of the plus-shape metamaterial is presented in Fig. 1b. The top view of the second design is presented in Fig. 1c. The light falls on the top of the metamaterial resonator. There is no ground plane used in this structure so the transmittance can also be considered while

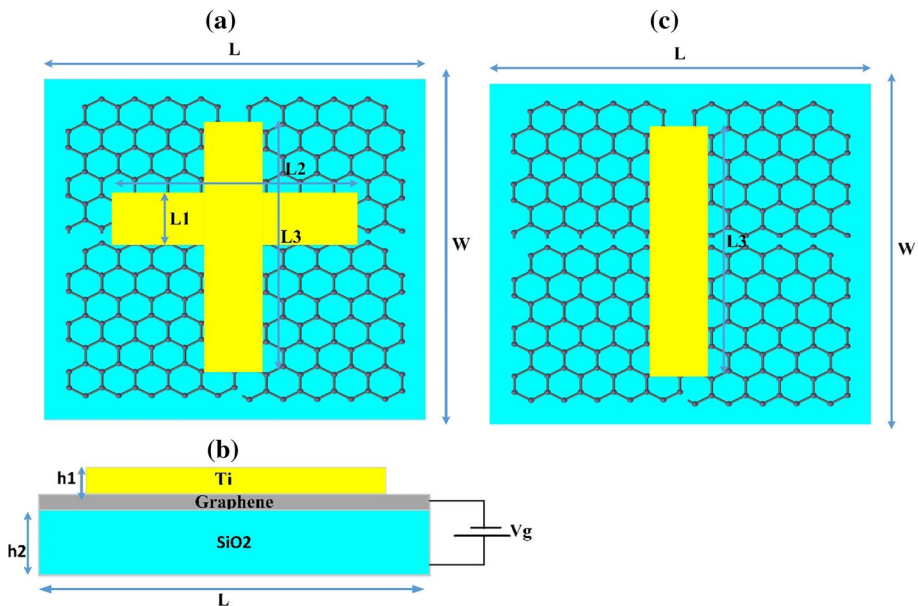


Fig. 1 Solar Absorber **a** Plus-shape design **b** front view of the plus shape design **c** I-shape design. The resonator thickness (h_1) is $0.2 \mu\text{m}$, substrate thickness (h_2) is $2.5 \mu\text{m}$. The length and width of the substrate is $2 \mu\text{m}$. The dimensions $L_1 = 120 \text{ nm}$, $L_2 = 920 \text{ nm}$ and $L_3 = 1560 \text{ nm}$. Graphene potential V_g is applied to graphene material. The figure is not drawn up to the scale

calculating absorption. We have applied the graphene potential and presented it in Fig. 1. The graphene potential is applied (Patel et al. 2020).

The graphene monolayer is used as a spacer for improving the results. The graphene conductivity is mainly based on the graphene potential (μ_c). The absorption behavior using the graphene layer and graphene potential effect on its conductivity is presented here in this section.

2.1 Graphene analysis

Graphene is a highly conducting material and its conductivity (σ_s) depends on graphene potential (μ_c). The equations below show this dependency which includes parameters like ($k_B = Boltzman\ constant$, $\Gamma = scattering\ rate$ and $T = room\ temperature$ Parmar et al. 2019). The graphene analysis using Kubo formula is presented and the results of absorption for various graphene chemical potentials are shown in the following section.

$$\varepsilon(\omega) = 1 + \frac{\sigma_s}{\varepsilon_0 \omega \Delta} \quad (1)$$

$$\sigma_{intra} = \frac{-je^2 k_B T}{\pi \hbar^2 (\omega - j2\Gamma)} \left(\frac{\mu_c}{k_B T} + 2 \ln \left(e^{-\frac{\mu_c}{k_B T}} + 1 \right) \right) \quad (2)$$

$$\sigma_{inter} = \frac{-je^2}{4\pi \hbar} \ln \left(\frac{2|\mu_c| - (\omega - j2\Gamma)\hbar}{2|\mu_c| + (\omega - j2\Gamma)\hbar} \right) \quad (3)$$

$$\sigma_s = \sigma_{inter} + \sigma_{intra} \quad (4)$$

2.2 Analysis of absorption

The absorption Eqs. (5–8) are analyzed in Surve et al. (2021). The equations show relation of angles (θ_i) and μ_c have also been resembled in the following sections in detail.

$$r(\omega, \theta_i) = \frac{\omega \cos \theta_i \prod_{00}(\omega, \theta_i)}{2i\hbar ck^2 + \omega \cos \theta_i \prod_{00}(\omega, \theta_i)} \quad (5)$$

$$\sigma_{||}(\omega, k) = -i \frac{\omega}{4\pi \hbar k^2} \prod_{00}(\omega, k) \quad (6)$$

$$r(\omega, \theta_i) = \frac{2\pi \cos \theta_i \sigma_{||}(\omega, k)}{c + 2\pi \cos \theta_i \sigma_{||}(\omega, k)} \quad (7)$$

$$\mathcal{R}(\omega, \theta_i) = |r(\omega, \theta_i)|^2 \quad (8)$$

$$\mathcal{R}(\omega, \theta_i) = \frac{4\pi^2 \cos^2 \theta_i [\text{Re}^2 \sigma_{||}(\omega, k) + \text{Im}^2 \sigma_{||}(\omega, k)]}{[c + 2\pi \cos \theta_i \text{Re} \sigma_{||}(\omega, k)]^2 + 4\pi^2 \cos^2 \theta_i \text{Im}^2 \sigma_{||}(\omega, k)} \tag{9}$$

$$\mathcal{R}(\omega) = \mathcal{R}(\omega, 0) = \frac{4\pi^2 [\text{Re}^2 \sigma(\omega) + \text{Im}^2 \sigma(\omega)]}{[c + 2\pi \text{Re} \sigma(\omega)]^2 + 4\pi^2 \text{Im}^2 \sigma(\omega)} \tag{10}$$

$$\text{Absorption} = 1 - \text{Reflectance} - \text{Transmittance} \tag{11}$$

3 Metasurface solar absorber results

Using the COMSOL Multiphysics simulation software, the metasurface designs shown in Fig. 1 are created to obtain its absorption response and electric field results. We have used periodic boundary conditions with Delaunay tessellation and plane wave source. Absorption is calculated by using Eq. 11 with periodic boundary conditions applied with Delaunay tessellation meshing conditions. Absorption results for plus-shape metamaterial design and I-shape metamaterial design are presented in Fig. 2. From the figure, it is clear that the plus-shape absorption result shown in the blue line is more compared to the I-shape results shown in the orange dash line. The absorption is provided for the range of 0.1 μm to 3 μm. The absorption is compared for visible region, ultraviolet region and infrared region in Table 1. The proposed structure shown in Fig. 1 can be experimentally tested using Chemical Vapour Deposition (CVD). Graphene monolayer deposition over substrate can

Fig. 2 **a** Comparison plot with absorption result for two metasurface designs. Performance-wise, the plus-shape design outperforms the I-shape design. **b** Reflectance, absorption and transmittance plot of plus-shape design

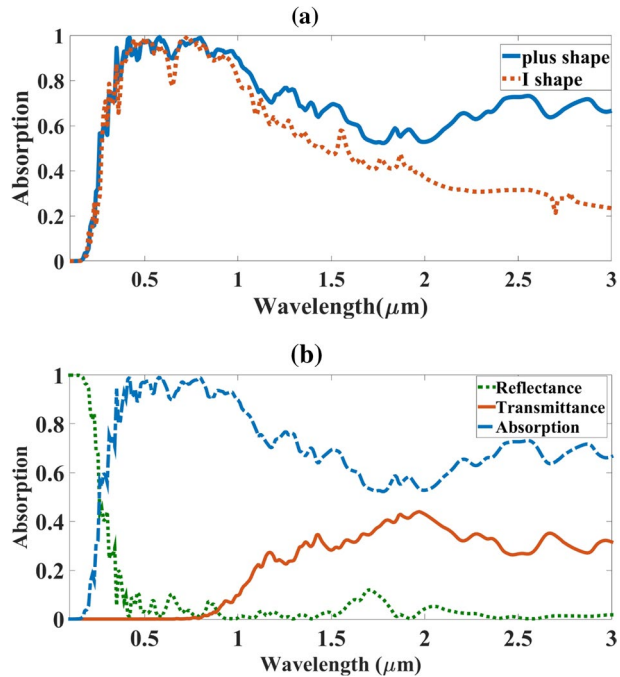


Table 1 Comparison between the designs

	UV region (0.2 to 0.4 μm) absorption (%)	Vis region (0.4 to 0.7 μm) absorption (%)	Infra region (0.7 to 1.2 μm) absorption (%)
Plus-shape design	61	95	88
I-shape design	58	93	83

be done with CVD and then gold layer can be deposited over graphene monolayer (Park et al. 2019).

The absorption response for different physical parameters like substrate thickness, substrate width, substrate length, resonator width, resonator thickness, angle of incidence and graphene potential is presented in Figs. 3, 4, 5.

Substrate thickness, Substrate length and Substrate width are key factors to consider while calculating the structure's absorption. The variation in these parameters can give the optimized design which has the highest absorption considering those parameters. The absorption results for different variations of substrate parameters are presented in Fig. 3. The length and width of the substrate are kept the same as the structure is a square shape. The unit cell structure is square so there should not be much difference in the results obtained in these two parameters. The substrate length and substrate width are varied from 2 to 5 μm as presented in Fig. 3a and b respectively. The variation in the results clearly shows that for substrate length and substrate width the increase in its values reduces the absorption values. The reduction in absorption occurs because of a change in resonance as the overall structure size is changing. This show that the smaller the periodic cell gives better absorption because the increase in periodic cell size with the same metasurface size changes the resonance and effects in a reduction in absorption. Because of all these reasons better absorption is visible at 2 μm substrate length and substrate width. The substrate thickness is also very important in achieving better absorption. The substrate thickness is varied from 1 to 2.5 μm . The increase in substrate thickness helps in achieving better absorption which is visible in Fig. 3c. The increase in substrate thickness is limited to a certain range because above that the inductance of the structure is changing and it affects the overall absorption results. The absorption values are better for 2.5 μm substrate thickness (Table 2).

The resonator made up of titanium material plays a vital role if its width and its thickness are varied. The variation in length changes the metasurface design which results in a change in absorption of the design. The absorption results for different variations of resonator parameters are presented in Fig. 4. The resonator thickness and resonator width are varied and their effect on absorption plot is presented in Fig. 4a and b respectively. The variation in the resonator thickness is carried out from 0.2 to 1 μm . The variation in the resonator thickness is not affecting much to the absorption results between 0.2 to 1.2 μm wavelength. The red color area clearly shows this response. This indicates that resonator thickness range is giving better inductance and resonance for those variations and thus good results are visible in the response. The variation in the width of plus-shape metasurface width is carried out from 40 to 120 nm. The results shown in Fig. 4b show that the absorption is better for higher widths. For the width of 120 nm the absorption is highest in the range of 0.2–1.2 μm and the other range also it is showing good absorption. The increase in width changes the resonance of the metasurface and it improves the absorption

Table 2 Comparison of the proposed designs with similar published designs from reference

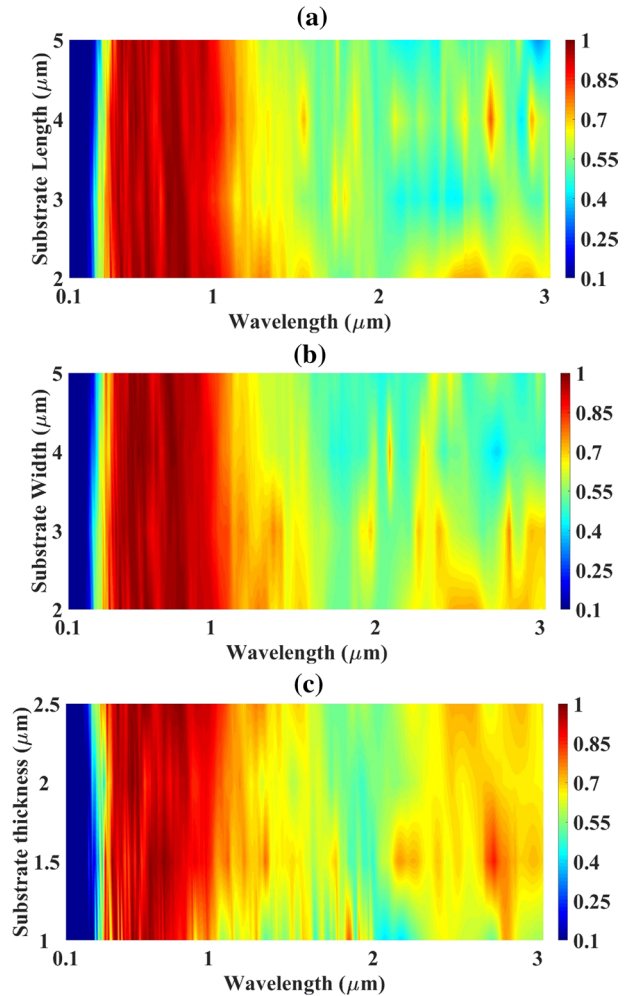
Design	UV region (0.2 to 0.4 μm) Absorption (%)	Vis Region (0.4 to 0.7 μm) Absorption (%)	Infra region (0.7 to 1.2 μm) Absorption (%)
Plus-shape design	61	95	88
I-shape design	58	93	83
From Patel et al. (2019c)	–	93.7	–
From Lin et al. (2019)	–	93	–
From Azad et al. (2016)	–	90	–
From Patel et al. (2020)	–	86.5	–
From Liu (2018)	–	80	–
From Sang et al. (2019)	–	71.1	–
From Rufangura and Sabah (2017)	–	70	–
From Yu et al. (2019)	–	90	–
From Cao and Cheng (2019)	–	90	–

as it is visible in the paper. The width of the plus-shape metasurface plays an important role as the thickness increase changes the overall resonance by changing the permittivity and permeability of the design.

The incident angle is important because solar energy is changing as the day progress. The different angles of incidence show the angular behavior of solar radiation during the day. The response should be available for the wide angle of incidence to be highly efficient. The absorption results for different variations of angle of incidence and graphene potential are presented in Fig. 5. The variation in the angle of incidence is carried out from 0° to 80° . The angle of incidence from 0° to 50° the absorption is good for most of the range. As the angle of incidence increases above 50° , the absorption reduces from the initial range of 0.2–1.2 μm . The graphene potential is varied from 0.1 to 0.9 eV for the wavelength range of 0.1–3 μm . The change is graphene chemical potential is not affecting the overall absorption for the whole wavelength range. The absorption is higher in the range of 0.2–1.2 μm wavelength range for all the graphene chemical potentials.

Electric field (EF) results are showing the concentration of normalized electric field in V/m. The more the electric field than more the absorption in that particular region. Electric field results are absorption is presented in Fig. 6 for wavelengths 0.2 μm , 0.5 μm , 0.8 μm , and 1.1 μm . The absorption is minimum for 0.2 μm and maximum for 0.5 μm . The EF results are showing good agreement with corresponding absorption values. The red color shows the highest EF and the blue part shows the minimum EF. The highest EF values are 7.5×10^7 V/m.

Fig. 3 Absorption results from variation in substrate length, substrate width and substrate thickness **a** Substrate length values of 2 to 5 μm **b** Substrate width values of 2 to 5 μm **c** Values for the substrate's thickness between 1 and 2.5 μm . The measured wavelengths are between 0.1 and 3 μm . The high absorption values are presented with red color and low absorption values are presented with blue color



4 Conclusion

The proposed absorber design is giving broadband absorption covering the visible region, ultraviolet region, and infrared region. The design results for the plus-shape metasurface design is showing better performance than the I-shape metasurface design. The plus-shape metasurface design is giving the highest average of 95% absorption in the visible region compared to 93% absorption of the I-shape metasurface design. The design results are also showing better performance compared with other published results. The physical parameters are also varied to obtain optimized results. The optimized design is having substrate width of 2 μm , substrate length of 2 μm , resonator thickness of 0.2 μm , resonator width of 120 nm, and substrate thickness of 2.5 μm . The EF results are also matching well with the obtained absorption results. The graphene potential is not affecting the overall absorption of the design. The wide angle of incidence is observed over 0° to 50° . The proposed solar absorber is applicable in converting solar radiation to thermal energy.

Fig. 4 **a** Resonator thickness values of 0.2 to 1 μm **b** Resonator width amounts of 40 to 120 nm. The wavelength examined is 0.1 to 3 μm . The high absorption values are presented with red color and low absorption values are presented with blue color

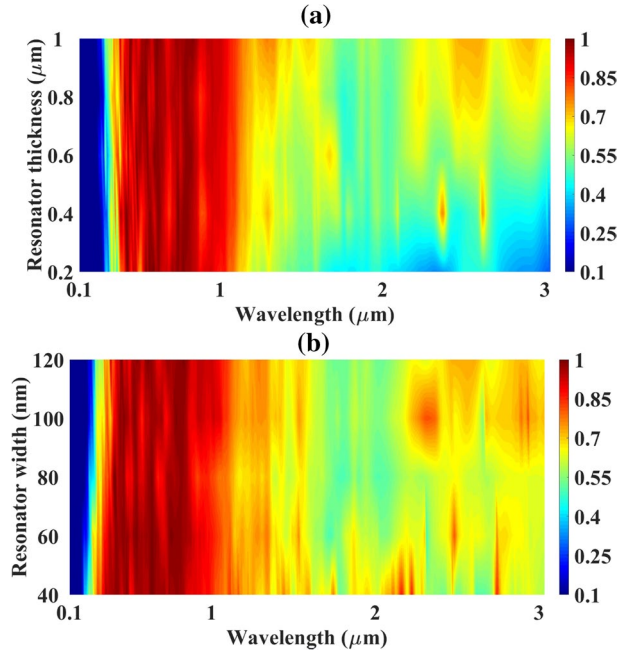
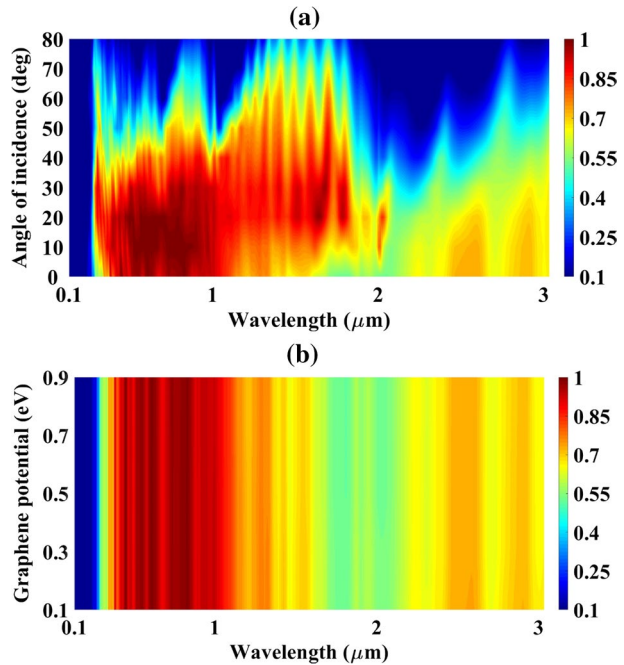


Fig. 5 Absorption results by variation in angle of incidence and graphene potential **a** Angle of incidence from 0 to 80 deg **b** Graphene potential values of 0.1 to 0.9 eV. The wavelength examined from 0.1 to 3 μm . The high absorption values are presented with red color and low absorption values are presented with blue color



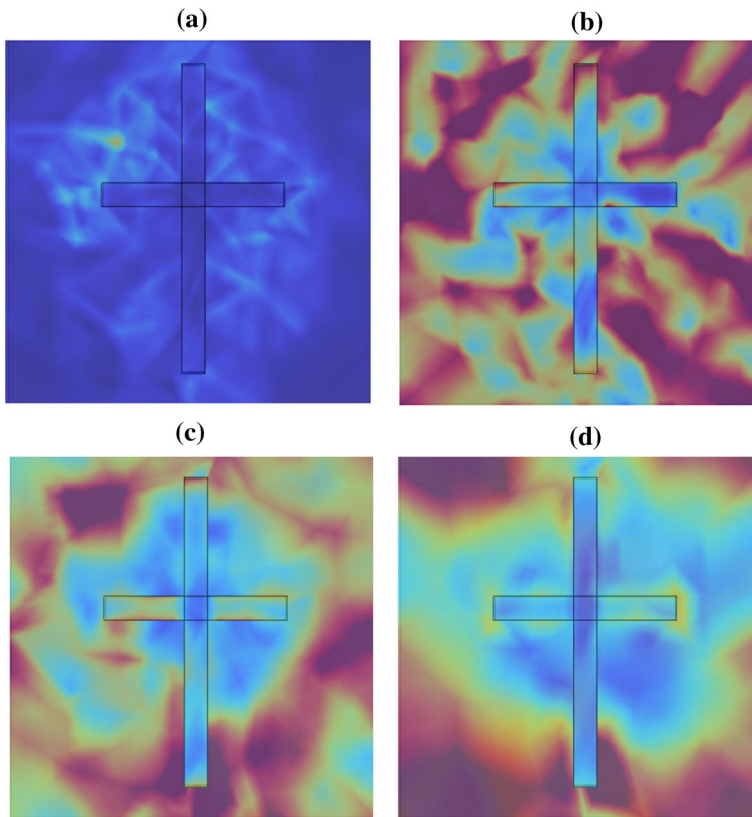


Fig. 6 EF of metasurface absorber for four different wavelengths **a** 0.2 μm **b** 0.5 μm **c** 0.8 μm **d** 1.1 μm . The EF is a minimum of around 0.2 μm which is also matching our absorption results. The highest EF values are 7.5×10^7 V/m presented with red color in the plot

Funding The authors have not disclosed any funding.

Data availability The data will be made available at a reasonable request to corresponding author.

Declarations

Conflict of interest Authors declare no conflict of interest.

References

- AL-Rjoub, A., Rebouta, L., Costa, P., Vieira, L.G.: Multi-layer solar selective absorber coatings based on for high temperature applications. *Sol. Energy Mater. Sol. Cells* (2018). <https://doi.org/10.1016/j.solmat.2018.07.001>
- Azad, A.K., et al.: Metasurface broadband solar absorber. *Sci. Rep.* (2016). <https://doi.org/10.1038/srep20347>
- Bait-Suwailam, M. M., Alajmi, H., and Masoud, M.: A Solar Energy Absorber Design Using Meta-material Particles for Renewable Energy Solutions, in *2019 2nd IEEE Middle East and North*

- Africa COMMunications Conference, MENACOMM 2019*, (2019). <https://doi.org/10.1109/MENACOMM46666.2019.8988580>.
- Bilal, R.M.H., Baqir, M.A., Choudhury, P.K., Naveed, M.A., Ali, M.M., Rahim, A.A.: Ultrathin broadband metasurface-based absorber comprised of tungsten nanowires. *Results Phys.* (2020). <https://doi.org/10.1016/j.rinp.2020.103471>
- Cao, C., Cheng, Y.: A broadband plasmonic light absorber based on a tungsten meander-ring-resonator in visible region. *Appl. Phys. A Mater. Sci. Process.* (2019). <https://doi.org/10.1007/s00339-018-2310-1>
- Charola, S., Patel, S.K., Parmar, J., Ladumor, M., Dhasarathan, V.: Broadband graphene-based metasurface solar absorber. *Microw. Opt. Technol. Lett.* **62**(3), 1366–1373 (2020). <https://doi.org/10.1002/mop.32156>
- Chen, F., Cheng, Y., Luo, H.: A broadband tunable terahertz metamaterial absorber based on single-layer complementary gammadion-shaped graphene. *Materials (Basel)* (2020). <https://doi.org/10.3390/ma13040860>
- Cheng, Y., Chen, F., Luo, H.: Multi-band giant circular dichroism based on conjugated bilayer twisted-semicircle nanostructure at optical frequency. *Phys. Lett. Sect. A Gen. at. Solid State Phys.* (2020). <https://doi.org/10.1016/j.physleta.2020.126398>
- Cheng, Y., Chen, F., Luo, H.: Plasmonic chiral metasurface absorber based on bilayer fourfold twisted semicircle nanostructure at optical frequency. *Nanoscale Res. Lett.* (2021a). <https://doi.org/10.1186/s11671-021-03474-6>
- Cheng, Y., Liu, J., Chen, F., Luo, H., Li, X.: Optically switchable broadband metasurface absorber based on square ring shaped photoconductive silicon for terahertz waves". *Phys. Lett. Sect. A Gen. at. Solid State Phys.* (2021b). <https://doi.org/10.1016/j.physleta.2021b.127345>
- Cheng, Y., Li, Z., Cheng, Z.: Terahertz perfect absorber based on InSb metasurface for both temperature and refractive index sensing. *Opt. Mater. (Amst)* (2021c). <https://doi.org/10.1016/j.optmat.2021.111129>
- Elavarasan, R.M., et al.: A comprehensive review on renewable energy development, challenges, and policies of leading indian states with an international perspective. *IEEE Access* **8**, 74432–74457 (2020). <https://doi.org/10.1109/ACCESS.2020.2988011>
- Feng, H., et al.: Tunable polarization-independent and angle-insensitive broadband terahertz absorber with graphene metamaterials. *Opt. Express* (2021). <https://doi.org/10.1364/oe.418865>
- Han, J., Chen, R.: Tunable broadband terahertz absorber based on a single-layer graphene metasurface. *Opt. Express* (2020). <https://doi.org/10.1364/oe.403631>
- Han, S., Shin, J.H., Jung, P.H., Lee, H., Lee, B.J.: Broadband solar thermal absorber based on optical metamaterials for high-temperature applications. *Adv. Opt. Mater.* (2016). <https://doi.org/10.1002/adom.201600236>
- Heidari, M.H., Sedighy, S.H.: Broadband wide-angle polarization-insensitive metasurface solar absorber. *J. Opt. Soc. Am. A* **35**(4), 522 (2018). <https://doi.org/10.1364/josaa.35.000522>
- Jadeja, R., et al.: Numerical investigation of graphene-based efficient and broadband metasurface for terahertz solar absorber. *J. Mater. Sci.* (2020). <https://doi.org/10.1007/s10853-019-04269-y>
- Li, J., et al.: Broadband solar energy absorber based on monolayer molybdenum disulfide using tungsten elliptical arrays. *Mater. Today Energy* (2020). <https://doi.org/10.1016/j.mtener.2020.100390>
- Lin, H., et al.: A 90-nm-thick graphene metamaterial for strong and extremely broadband absorption of unpolarized light. *Nat. Photonics* (2019). <https://doi.org/10.1038/s41566-019-0389-3>
- Liu, B., et al.: Multiband and broadband absorption enhancement of monolayer graphene at optical frequencies from multiple magnetic dipole resonances in metamaterials. *Nanoscale Res. Lett.* (2018). <https://doi.org/10.1186/s11671-018-2569-3>
- Mehrabi, S., Rezaei, M.H., Zarifkar, A.: Ultra-broadband metamaterial absorber based on cross-shaped TiN resonators. *J. Opt. Soc. Am. A* **37**(4), 697–704 (2020). <https://doi.org/10.1364/josaa.389320>
- Park, Y., Koo, J.Y., Kim, S., Choi, H.C.: Spontaneous formation of gold nanoparticles on graphene by galvanic reaction through graphene. *ACS Omega* (2019). <https://doi.org/10.1021/acsomega.9b02691>
- Parmar, J., Patel, S.K.: Encrypted and tunable graphene-based metasurface refractive index sensor. *Microw. Opt. Technol. Lett.* (2021). <https://doi.org/10.1002/mop.33049>
- Parmar, J., Patel, S.K., Ladumor, M., Sorathiya, V., Katrodiya, D.: Graphene-silicon hybrid chirped-superstructure bragg gratings for far infrared frequency. *Mater. Res. Express* (2019). <https://doi.org/10.1088/2053-1591/ab0b5d>
- Parmar, J., Patel, S.K., Katkar, V.: Graphene-based metasurface solar absorber design with absorption prediction using machine learning. *Sci. Rep.* **12**(1), 1–11 (2022). <https://doi.org/10.1038/s41598-022-06687-6>
- Patel, S.K., Ladumor, M., Parmar, J., Guo, T.: Graphene-based tunable reflector superstructure grating. *Appl. Phys. A Mater. Sci. Process.* (2019a). <https://doi.org/10.1007/s00339-019-2872-6>

- Patel, S.K., Charola, S., Jani, C., Ladumor, M., Parmar, J., Guo, T.: Graphene-based highly efficient and broadband solar absorber. *Opt Mater (Amst)* **96**, 109330 (2019b). <https://doi.org/10.1016/j.optmat.2019b.109330>
- Patel, S.K., Charola, S., Parmar, J., Ladumor, M.: Broadband metasurface solar absorber in the visible and near-infrared region. *Mater. Res. Express* (2019c). <https://doi.org/10.1088/2053-1591/ab207d>
- Patel, S.K., Charola, S., Parmar, J., Ladumor, M., Ngo, Q.M., Dhasarathan, V.: Broadband and efficient graphene solar absorber using periodical array of C-shaped metasurface. *Opt. Quantum Electron.* **126**(5), 1–16 (2020). <https://doi.org/10.1007/s11082-020-02379-5>
- Patel, S.K., Sorathiya, V., Lavadiya, S., Luo, Y., Nguyen, T.K., Dhasarathan, V.: Numerical analysis of polarization-insensitive squared spiral-shaped graphene metasurface with negative refractive index. *Appl. Phys. B Lasers Opt.* (2020). <https://doi.org/10.1007/s00340-020-07435-2>
- Patel, S., Parmar, J., Katrodiya, D., Nguyen, T.K., Holdengreber, E., Dhasarathan, V.: Broadband metamaterial-based near-infrared absorber using array of uniformly placed gold resonators. *J Opt Soc Am B* **37**(7), 2163 (2020). <https://doi.org/10.1364/josab.389283>
- Patel, S.K., Surve, J., Parmar, J., Nguyen, T.K.: Review on graphene-based absorbers for infrared to ultraviolet frequencies. *J. Adv. Eng. Comput.* (2021a). <https://doi.org/10.55579/jaec.202154.350>
- Patel, S.K., Parmar, J., Zakaria, R.B., Sharafali, A., Nguyen, T.K., Dhasarathan, V.: Sensitivity analysis of metasurface array-based refractive index biosensors. *IEEE Sens. J.* (2021b). <https://doi.org/10.1109/JSEN.2020.3017938>
- Patel, S.K., Parmar, J., Katkar, V.: Metasurface-based solar absorber with absorption prediction using machine learning. *Opt. Mater. (Amst)* **124**, 112049 (2022). <https://doi.org/10.1016/j.optmat.2022.112049>
- Rahmanzadeh, M., Rajabalipanah, H., Abdolali, A.: Multilayer graphene-based metasurfaces: robust design method for extremely broadband, wide-angle, and polarization-insensitive terahertz absorbers. *Appl. Opt.* (2018). <https://doi.org/10.1364/ao.57.000959>
- Rufangura, P., Sabah, C.: Dual-band perfect metamaterial absorber for solar cell applications. *Vacuum* **120**, 68–74 (2015). <https://doi.org/10.1016/j.vacuum.2015.05.033>
- Rufangura, P., Sabah, C.: Graphene-based wideband metamaterial absorber for solar cells application. *J. Nanophotonics* **11**(3), 036008-1–036008-9 (2017). <https://doi.org/10.1117/1.jnp.11.036008>
- Sang, T., Gao, J., Yin, X., Qi, H., Wang, L., Jiao, H.: Angle-insensitive broadband absorption enhancement of graphene using a multi-grooved metasurface. *Nanoscale Res. Lett.* (2019). <https://doi.org/10.1186/s11671-019-2937-7>
- Surve, J., Parmar, J., Patel, S.K., Jadeja, R.: Comparative analysis of metasurface array-based solar absorber for visible region. *Opt. Quantum Electron.* **53**(12), 1–22 (2021). <https://doi.org/10.1007/s11082-021-03355-3>
- Te Lin, K., Lin, H., Yang, T., Jia, B.: Structured graphene metamaterial selective absorbers for high efficiency and omnidirectional solar thermal energy conversion. *Nat. Commun.* (2020). <https://doi.org/10.1038/s41467-020-15116-z>
- Torabi, E.S., Fallahi, A., Yahaghi, A.: Evolutionary optimization of graphene-metal metasurfaces for tunable broadband terahertz absorption. *IEEE Trans. Antennas Propag.* **65**(3), 1464–1467 (2017). <https://doi.org/10.1109/TAP.2016.2647580>
- Wang, H., Prasad Sivan, V., Mitchell, A., Rosengarten, G., Phelan, P., Wang, L.: Highly efficient selective metamaterial absorber for high-temperature solar thermal energy harvesting. *Sol. Energy Mater. Sol. Cells* **137**, 235–242 (2015). <https://doi.org/10.1016/j.solmat.2015.02.019>
- Xu, H., Hu, L., Lu, Y., Xu, J., Chen, Y.: Dual-band metamaterial absorbers in the visible and near-infrared regions. *J. Phys. Chem. C* **123**(15), 10028–10033 (2019). <https://doi.org/10.1021/acs.jpcc.9b00434>
- Yu, P., et al.: A numerical research of wideband solar absorber based on refractory metal from visible to near infrared. *Opt. Mater. (Amst)* (2019). <https://doi.org/10.1016/j.optmat.2019.109400>
- Zhang, H., Cheng, Y., Chen, F.: Quad-band plasmonic perfect absorber using all-metal nanostructure metasurface for refractive index sensing. *Optik (Stuttg)* (2021). <https://doi.org/10.1016/j.jilleo.2021.166300>
- Zhang, J., Wang, C., Shi, J., Wei, D., Zhao, H., Ma, C.: Solar selective absorber for emerging sustainable applications. *Adv. Energy Sustain. Res.* (2022). <https://doi.org/10.1002/aesr.202100195>

Publisher's Note Springer Nature remains neutral with regard to jurisdictional claims in published maps and institutional affiliations.

Springer Nature or its licensor holds exclusive rights to this article under a publishing agreement with the author(s) or other rightsholder(s); author self-archiving of the accepted manuscript version of this article is solely governed by the terms of such publishing agreement and applicable law.